00320

A CONSTITUTIVE MODEL FOR SIMULATING VISCOELASTIC RESPONSE FROM HIGH DAMPING RUBBER

A.F.M.S. Amin[1], M.S. Alam[2], S.I. Wiraguna[3] and Y. Okui[4]

1) Department of Civil and Environmental Engineering, Saitama University
255 Shimo Okubo, Saitama-shi, Saitama 338-8750, Japan
E-mail: amin@koz.struct.civil.saitama-u.ac.jp
2) Department of Civil and Environmental Engineering, Saitama University
255 Shimo Okubo, Saitama-shi, Saitama 338-8750, Japan
E-mail: alam@koz.struct.civil.saitama-u.ac.jp
3) Department of Civil and Environmental Engineering, Saitama University
255 Shimo Okubo, Saitama-shi, Saitama 338-8750, Japan
E-mail: sena@koz.struct.civil.saitama-u.ac.jp
4) Department of Civil and Environmental Engineering, Saitama University
255 Shimo Okubo, Saitama-shi, Saitama 338-8750, Japan
E-mail: okui@koz.struct.civil.saitama-u.ac.jp

ABSTRACT

The characteristic viscoelastic effect exhibited by high damping rubber (HDR) was investigated in compression. The presence of strain-rate dependent high stiffness at low compressive strain became evident from the investigation. A hyperelasticity model was proposed to represent the rate-independent elastic response including the high initial stiffness feature. The model was incorporated in a finite deformation rate-dependent model structure. A physically meaningful parameter identification scheme proposed in Amin et al. (2001) was employed to identify the elasticity and viscosity parameters from experimental data. The adequacy of the proposed model and the parameter identification scheme was verified from the numerical simulation of test results.

INTRODUCTION

The use of high damping rubber (HDR) bearings as base isolation device has now become an accepted practice for protecting structures from earthquakes (Kelly, 1997). Unlike natural rubbers (NR), quite a large amount of filler is usually added during vulcanization process to produce HDR (Dorfmann and Burtscher, 2000). The large filler content in the material provides high stiffness at low deformation level along with the significant increase in the strain-rate dependency characteristics. In this context, the major focus of this research was concentrated on developing a constitutive model that will be capable of simulating the rate-dependent response of HDR. Evidently, such a model should also be able to represent the high initial stiffness feature of the material.

Figure 1 presents a schematic representation of typical rate-dependent responses obtained from a viscoelastic solid. When a viscoelastic solid is loaded at an infinitely slow rate, the stress-strain curve follows the E-E' path. This behavior is called the equilibrium response. On the other hand, in case of an infinitely fast loading rate, the response takes the I-I' path. Such a response is known as the instantaneous response. Both equilibrium and instantaneous responses are elastic responses and the domain of viscosity lies in between these two states (Huber and Tsakmakis, 2000). Hence, one of the ways of developing a physically meaningful constitutive model is to include parameters that will directly express the instantaneous and equilibrium response of the material.

In this context, a standard three parameter parallel model as illustrated in Fig. 2 can be considered where the first branch comprising of a spring (Element A) can represent the equilibrium response while the second branch comprising of a spring (Element B) and a dashpot (Element C) can represent the 'overstress' feature resulting from the rate-dependent effect. However, in contrast to the models of linear viscoelasticity, nonlinear spring elements are required to represent the nonlinear equilibrium and instantaneous responses. In this context, use of an adequate hyperelasticity formulation is vital (Bonet and Wood, 1997). Furthermore, in ideal cases, monotonic tests with infinitely fast and slow rates are required to identify the

elastic boundary parameters. However, specially in case of highly viscous material like HDR, there are experimental limitations in applying such extreme loading rates to arrive either at the instantaneous state or the equilibriums state for identifying the material parameters. In this context, the process conventionally followed is to perform some extensive numerical trials to estimate these parameters (Lion, 1997). However, the parameters identified in this way lose the physical meaning.

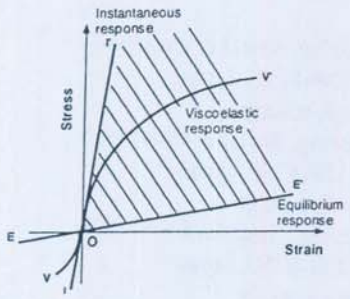

Fig. 1. Typical responses from a viscoelastic solid.

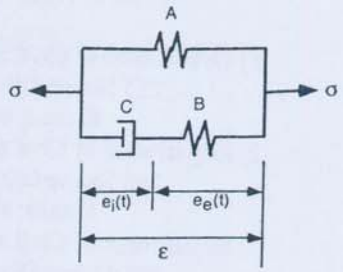

Fig. 2. A three-parameter representation of viscoelastic effect

With this background, experiments were carried out to observe the fundamental viscoelastic response of HDR in compression. On the basis of the experimental observation, an improved hyperelasticity function was proposed to represent the rate-independent elastic response. In order to simulate the rate-dependent response, the function was incorporated in a rate-dependent finite deformation model structure. The parameter identification scheme proposed by Amin et al. (2001) for NR was employed to estimate the elasticity and viscosity parameters from experimental data. The numerical simulation of test results in compression and tension regime substantiated the adequacy of the proposed model.

EXPERIMENTS

An experimental scheme comprising of a multi-step relaxation test, monotonic compression tests and simple relaxation tests were carried out to observe the fundamental viscoelastic behavior of HDR characterized by equilibrium response, instantaneous response and viscosity effect (Figure 1). In order to remove the Mullins' effect from other inelastic phenomena, a 5-cycle preloading sequence was applied on the specimens prior to the actual tests. The details of the experimental set-up and conditions are available in our earlier communication (Amin et al. 2001) that deals with NR behavior.

The equilibrium response defined in Fig. 1 can ideally be obtained when the material is loaded at an infinitely slow rate. However, in case of a highly viscous material like HDR, it is difficult to specify a loading rate that will be slow enough to rule out the viscosity effect. To over come this problem, a multi-step relaxation test with multiple hold-times over the considered stretch (i.e. 1+dL/L, where L is the undeformed length) range was proposed. Figure 3 presents the applied stretch and resultant stress histories obtained in compression regime. The figure clarifies the asymptotic convergence of the stress history at the end of each relaxation interval indicating the stresses to reach the neighborhood of equilibrium state.

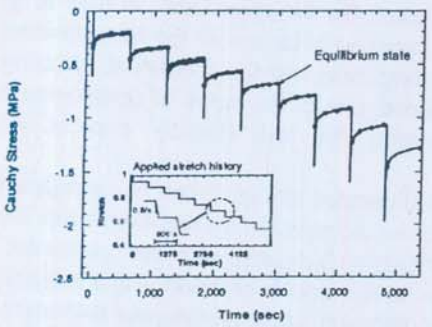

Fig. 3. Applied stretch history and stretch-stress response observed in multi-step relaxation test.

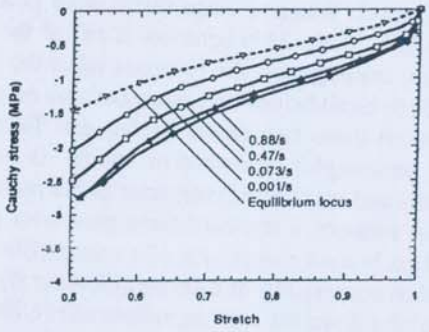

Fig. 4. Monotonic compression test stretch-stress responses at different strain rates and equilibrium locus.

Figure 1 has defined the instantaneous response from a material that can be obtained if the material is loaded at infinitely fast loading rate. However, there are practical limitations to apply such extreme loading condition on a specimen. In this situation, monotonic compression tests at different strain rates within the range of 0.001/s to 0.88/s were carried out. Figure 4 presents the stress-stretch responses that were observed in 4 strain rate cases. The strain-rate dependent high initial stiffness of HDR each of the responses is clearly visible. A further comparison between the different strain-rate cases indicates the increase of stress response with the increase of strain rate. This must be due to the viscosity effect. In addition, a diminishing trend in the increase of response can also be noticed at higher strain-rate cases indicating the approach of an instantaneous state. This conforms to our earlier observation on NR. The equilibrium locus obtained from multi-step relaxation test (Fig. 3) is plotted here to clarify the viscous domain. In addition, simple relaxation tests were also performed to clarify the viscosity effect.

CONSTITUTIVE MODEL

Classically, hyperelasticity laws are employed to represent the response of rubbers at a particular strain rate assuming the complete elastic recovery of the material (Bonet and Wood, 1997). In hyperelasticity, under the assumption of isotropy, the stress-strain relationship is derived from a strain energy density function, W that is expressed either in terms of strain invariants or principal stretches. In the first approach, the three strain invariants (I_1, I_2, I_3) are expressed as:

$$\begin{aligned} I_1 &= \mathrm{tr}\mathbf{B} = \lambda_1^2 + \lambda_2^2 + \lambda_3^2, \\ I_2 &= \frac{1}{2}\left\{(\mathrm{tr}\mathbf{B})^2 - \mathrm{tr}(\mathbf{BB})\right\} = (\lambda_1\lambda_2)^2 + (\lambda_2\lambda_3)^2 + (\lambda_3\lambda_1)^2 \\ I_3 &= \det\mathbf{B} = (\lambda_1\lambda_2\lambda_3)^2, \end{aligned} \tag{1}$$

where λ_1, λ_2 and λ_3 are the stretches in the three principal directions, left Cauchy-Green deformation tensor, $\mathbf{B}=\mathbf{F}\mathbf{F}^T$ and $\mathbf{F}$ is the deformation gradient tensor. Under the assumption of incompressibility, I_3 reduces to unity allowing the other two invariants to describe W. However, according to Lambert-Diani and Rey (1999), it was concluded that only I_1 is sufficient to represent the uniaxial response. This conclusion was adopted in the current research to improve Yamashita and Kawabata (1992) model and thereby incorporate the initial stiffness feature representation. Equations (2) presents the proposed strain energy density function and the corresponding Cauchy stress expression where, C_5, C_3, C_4, M, N are material parameters with $N \geq 1.0$ and $M<1.0$.

$$\begin{aligned} W(I_1) &= C_5(I_1-3) + \frac{C_3}{N+1}(I_1-3)^{N+1} + \frac{C_4}{M+1}(I_1-3)^{M+1}, \\ \sigma_{11} &= 2\left(\lambda^2-\frac{1}{\lambda}\right)\left[C_5 + C_3(I_1-3)^N + C_4(I_1-3)^M\right] \end{aligned} \tag{2}$$

However, in order to model the viscoelastic effect, hyperelasticity laws are required to be combined with a rate-dependent model through a finite deformation model structure. To this end, the rheological model presented in Fig. 2 was converted into the finite deformation model following the formulation of Huber and Tsakmakis (2000). Each spring element was first modeled using the proposed hyperelasticity relation. Linearity was assumed for the viscosity represented by the dashpot. The finite deformation model was formulated under the framework of multiplicative decomposition of the deformation gradient tensor, $\mathbf{F}$. The total deformation gradient tensor was decomposed into $\mathbf{F}=\mathbf{F}_e\mathbf{F}_i$ where $\mathbf{F}_e$ and $\mathbf{F}_i$ are the deformation gradients associated with e_e and e_i respectively. This leads the following expressions for the Cauchy stress ($\mathbf{T}$) and rate of $\mathbf{B}_e$:

$$\begin{aligned} \mathbf{T} &= -p\mathbf{1} + 2C_5^{(E)}\mathbf{B} + 2C_3^{(E)}(I_{1B}-3)^{N^{(E)}}\mathbf{B} + 2C_4^{(E)}(I_{1B}-3)^{M^{(E)}}\mathbf{B} + \\ &\qquad 2C_5^{(OE)}\mathbf{B}_e + 2C_3^{(OE)}(I_{1B}-3)^{N^{(OE)}}\mathbf{B}_e + 2C_4^{(OE)}(I_{1B}-3)^{M^{(OE)}}\mathbf{B}_e \\ \dot{\mathbf{B}}_e &= \mathbf{B}_e\mathbf{L}^T + \mathbf{L}\mathbf{B}_e - \frac{4}{\eta}\mathbf{B}_e\left(C_5^{(OE)}\mathbf{B}_e + C_3^{(OE)}(I_{1B}-3)^{N^{(OE)}}\mathbf{B}_e + C_4^{(OE)}(I_{1B}-3)^{M^{(OE)}}\mathbf{B}_e\right)^D \end{aligned} \tag{3}$$

where, p is the hydrostatic pressure of $\mathbf{T}$, $\mathbf{1}$ is the identity tensor, subscript e denotes the quantities related to $\mathbf{F}_e$, superscript (E) denotes the equilibrium part represented by the first branch, the superscript (OE) denotes the overstress part represented by the second branch (Fig. 2), $\mathbf{L}$ is the velocity gradient tensor and η is the viscosity parameter. The parameter identification scheme published in Amin et al. (2001) was applied to identify the elastic and viscosity parameters for the above model.

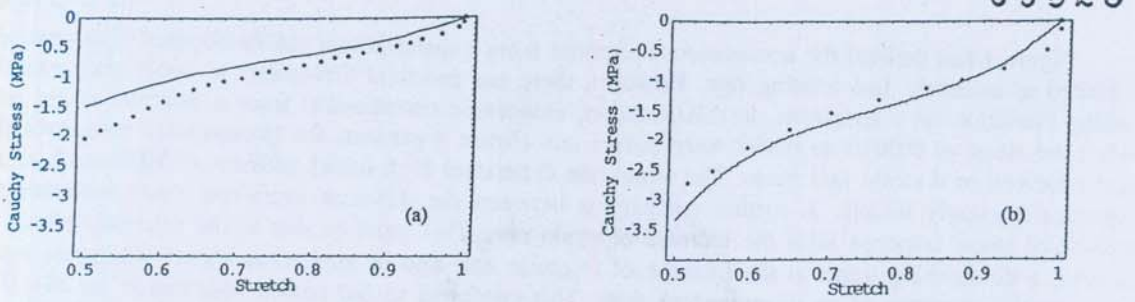

Fig. 4. Numerical simulation of monotonic compression test at different strain rates; (-) Numerical simulation, (•) Experiment. (a) 0.001/s (b) 0.88/s strain rates.

NUMERICAL SIMULATION

The capability of the model was verified through the numerical simulation of test results. Figure 8 presents the two strain-rate cases of monotonic compression test simulation. The comparison of the numerical results with experiments illustrates the model capability simulating the strain-rate dependent high initial stiffness. However, at the slower strain rate case, the representation is a bit poorer. This might be due to the limitations of the present viscoelasticity modeling where linear material viscosity was assumed.

CONCLUSIONS

Experiments were carried out to characterize the viscoelastic effect of HDR described by equilibrium response, instantaneous response and viscosity effect. An improved hyperelasticity relation was proposed and subsequently incorporated in a finite deformation rate-dependent model to derive a constitutive model capable of simulating the viscoelastic response of HDR. The parameter identification scheme proposed by the authors on NR was found applicable for HDR as well. Numerical simulation of test results has displayed the adequacy of the model and the applicability of the applicability of the parameter identification scheme.

ACKNOWLDGEMENTS

It is the pleasure for the authors to express deep gratitude to Professor H. Horii, Department of Civil Engineering, The University of Tokyo, Japan for extending experimental facilities of his laboratory to carry out the mechanical tests. Sincere acknowledgements also go to the Yokohama Rubber Company, Japan for providing test specimens.

REFERENCES

Amin, A. F. M. S., Alam, M. Shah and Okui, Y. (2001), Nonlinear Viscoelastic Response of Elastomers: Experiments, Parameter Identification and Numerical Simulation, *J. Struct. Engrg, JSCE,* 47A, pp. 181-192.

Dorfmann, A. and Burtscher, S. L. (2000), Aspects of Cavitation Damage in Seismic Bearings, *J. Struct. Engrg., ASCE,* 126, pp. 573-579.

Huber, N. and Tsakmakis, C. (2000), Finite deformation viscoelasticity laws, *Mech. Mater.,* 32, pp. 1-18.

Kelly, J. M. (1997), *Earthquake Resistant Design with Rubber*, Springer-Verlag, London.

Lambert-Diani, J. and Rey, C. (1999), New Phenomenological Behavior Laws for Rubbers and Thermo plastic Elastomers, *Eur. J. Mech. A/Solids*, 18, pp. 1027-1043.

Lion, A. (1997), A physically based method to represent the thermo-mechanical behavior of elastomers, *Acta Mechanica*, 123, pp. 1-25.

Yamashita, Y. and Kawabata, S. (1992), Approximated form of the strain energy density function of carbon-black filled rubbers for industrial applications, *J. Soc. Rubber Ind. (Jpn),* 65, pp. 517-528. *(In Japanese).*